

University of Arkansas, Fayetteville

ScholarWorks@UARK

Civil Engineering Undergraduate Honors Theses

Civil Engineering

5-2015

Analyzing stochastically generated material properties for the use in numerical simulations of advanced laboratory tests of asphalt concrete

Ken K. Rutabana

University of Arkansas, Fayetteville

Follow this and additional works at: <https://scholarworks.uark.edu/cveguht>



Part of the [Civil Engineering Commons](#), and the [Structural Engineering Commons](#)

Citation

Rutabana, K. K. (2015). Analyzing stochastically generated material properties for the use in numerical simulations of advanced laboratory tests of asphalt concrete. *Civil Engineering Undergraduate Honors Theses* Retrieved from <https://scholarworks.uark.edu/cveguht/25>

This Thesis is brought to you for free and open access by the Civil Engineering at ScholarWorks@UARK. It has been accepted for inclusion in Civil Engineering Undergraduate Honors Theses by an authorized administrator of ScholarWorks@UARK. For more information, please contact scholar@uark.edu, uarepos@uark.edu.

An Undergraduate Honors College Thesis

in the

College of Engineering
University of Arkansas
Fayetteville, AR


by

This thesis is approved.

Thesis Advisor:

 ANDREW F. BRAHAM

Thesis Committee:

 MICHAEL HALE

 Michelle L. Bernhardt

INTRODUCTION

Asphalt is and has been a very widely used construction material. It covers over 4 million miles of roadway in the United States alone and has been the subject of scientific research. There are many factors that quantify construction materials commonly used and asphalt is no different. Over the years countless performance tests have been developed and utilized to gauge and qualify asphalt and make sure it meets the necessary requirements. However, many of these tests are lengthy and expensive. Numerical simulations have long been used to keep testing procedure as minimal and efficient as possible. However, many of them do not account for the heterogeneous nature of asphalt's internal structure. In this experiment, three performance tests will be carried out on numerous asphalt samples. The results of these tests along with the sample properties representative of their internal structure (i.e. the air voids) will be used in the calibration of a numerical model. Using stochastic methods and finite element modeling and simulation techniques, this model will attempt to account for the uncertainty and variability that exists with performance testing. Furthermore, the high number of tests results generated from this project will provide an insight into the potential variability in results from these tests.

MATERIALS AND METHODS

The material used in this project was a 12.5mm Nominal Maximum Aggregate Size (NMAS) asphalt concrete mixture used in Lane 1 from the Federal Highway Administration Accelerated Loading Facility project. The asphalt binder was an unmodified PG64-22. The samples were obtained pre-mixed, and were compacted at two different temperatures: 144°F and 266°F. Due to the different compaction temperatures, the two sets of asphalt samples had different air voids contents which is a key variable when analyzing test results. Table 1 shows the mix design properties.

Table 1 – Asphalt concrete mix design

Dimension (mm)	Sieve Size	Sieve Size ^{0.45}	Approved Mix Design				
			General Limits		Job Mix Formula Range		Target Value
			Bottom	Up	Bottom	Up	
37.5	1 1/2 inch	5.11	100	100	100	100	100
25	1 inch	4.26	100	100	100	100	100
19	3/4 inch	3.76	100	100	100	100	100
12.5	1/2 inch	3.12	90	100	90	100	97
9.5	3/8 inch	2.75		90	82	90	86
4.75	# 4	2.02			41	55	48
2.36	# 8	1.47	28	58	26	34	30
1.18	# 16	1.08			18	24	21
0.6	# 30	0.79			13	19	16
0.3	# 50	0.58			9	15	12
0.15	# 100	0.43					8
0.075	#200	0.31	3	8	4	8	6
Design Mix Requirements			Parameter		Tolerance		Target
			G _{mm}	+0.015	-0.015	2.735	
			Air Voids	+1%	-1%	4.0	
			G _{mb}	+0.044	-0.044	2.632	
			G _{sb}	---		2.979	
			P _{ba}	+0.2	-0.2	5.00	
			VMA	>14		15.7	
			VFA	65	78	76.7	
			DB Ratio	0.6	1.8	1.2	

Sixteen asphalt concrete pucks were compacted using the mix design in Table 1. Eight samples were compacted at 144°F while the other eight were compacted at 266°F. In order to meet size and shape requirements for the three performance tests to be carried out, the sixteen specimens were cut and two “disks” were obtained from each puck. These cylindrical disks had a diameter of 150mm and an average height of 35.4mm, as seen in Figure 1. This is a deviation from the specifications that call for a minimum height of 38mm. Once again, the original pucks were too small to meet this requirement. However, extracting two samples from each puck allowed for the two samples to have a similar air void structure, as samples from the gyratory compactor are often symmetric along the axis. By trimming the edges, it was assumed that the two disks extracted from each puck had a similar air void structure. Since air voids were a crucial parameter in interpreting the data, the sample’s bulk specific gravity was measured using AASHTO T 331. Once the air voids were found, performance testing began on the specimens.

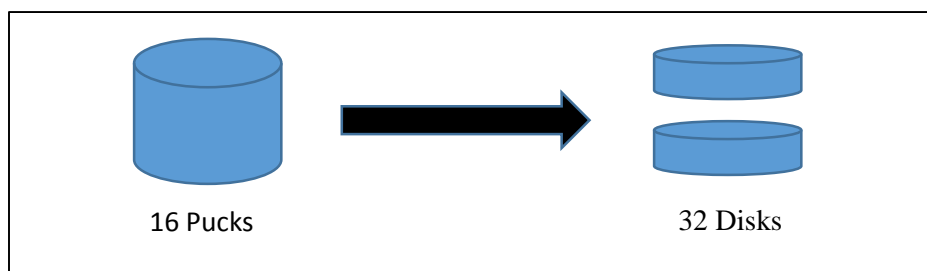


Figure 1 – From individual puck to disks

IDT Creep Test (AASHTO T322)

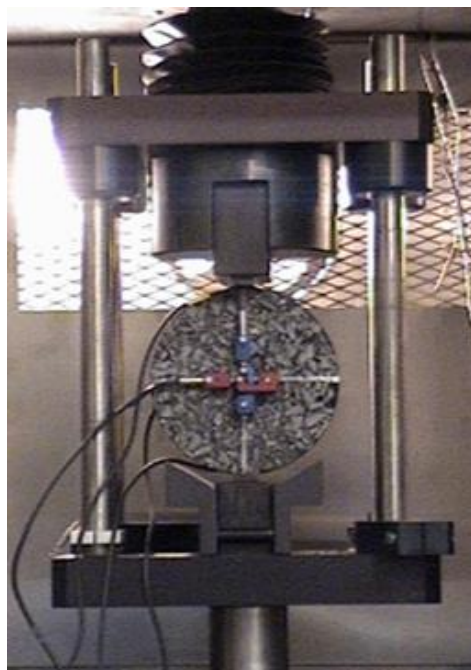


Figure 2 – IDT creep test (AASHTO T322, from <http://cait.rutgers.edu>)

All 32 slices were paired with their corresponding slice from the same puck and underwent the IDT Creep Test as described in AASHTO T322 and seen in Figure 2. However, there was one significant deviation from the specification. The AASHTO specification calls for three replicate slices from a single asphalt puck (six faces) to be tested together instead of the two slices (four faces) used in this experiment. The number of slices used was reduced from three to two because of the short height of the asphalt pucks. The specification further requires that the data be trimmed down from the six faces to four faces. This step was also not applied in this experiment and instead the four original faces were kept untrimmed. Once all the slices were tested, the top and bottom outlying set of two slices were trimmed out. The fourteen remaining pairs were then divided into 28 SC(B) tests and 14 IDT Strength tests.

Semi-Circular Bend [SC(B)] Fracture Test:

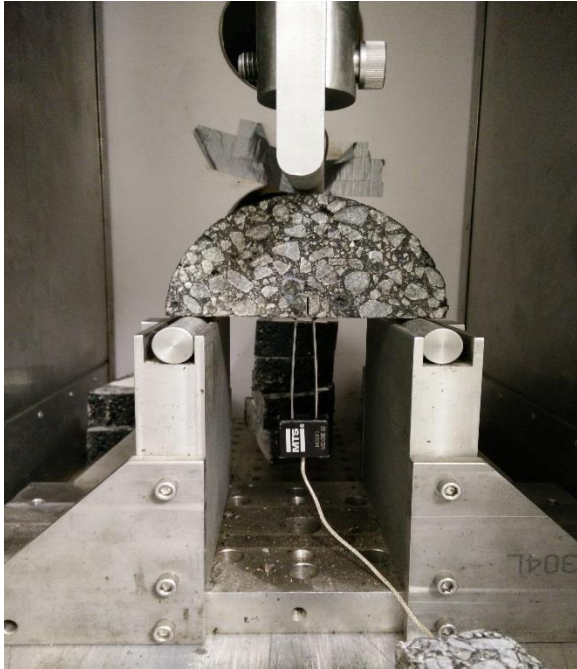


Figure 3 – Semi-Circular Bend [SC(B)] fracture test (AASHTO TP105)]

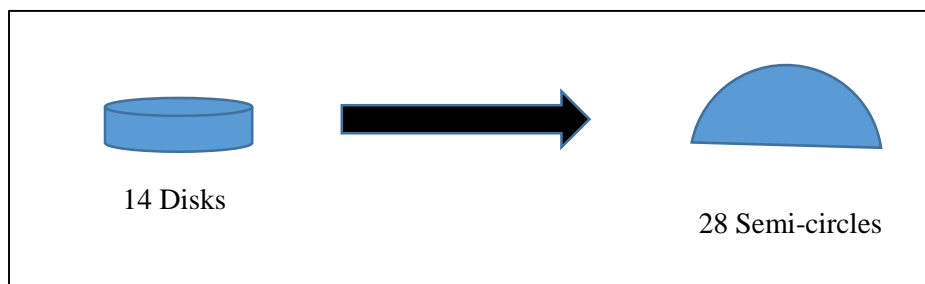


Figure 4 – From disks to semi-circles

The SC(B) test, in Figure 3, following AASHTO TP315, was carried out on seven of the untrimmed pairs. Additional specimen modification was required in order to meet the dimension requirements for the test. Each slice was cut in half along its diameter to produce two half-moon shaped samples as seen in Figure 4. A 15mm notch was then cut perpendicular to the previous cut. This notch creates a weak point in the specimen which will be the origin of the failure path. AASHTO T 331 was once again carried out to determine the individual air voids before the testing began. Unlike the IDT Creep test, the SC(B) test is a destructive test. Once the samples were tested, measurements of the cracking area of the failure plane surface area were collected. The cracking area is seen in Figure 5.



Figure 5 – SC(B) tested sample.

IDT Strength Test:



Figure 6 – Indirect Tensile Strength Test (AASHTO T322, from <https://engineering.purdue.edu/>)

The IDT strength test is very similar to the IDT Creep test and also follows AASHTO T322, as seen in Figure 6. The test specimens are of the same dimension and are

loaded in a similar manner. The main difference between the two tests however, is that the strength test is a destructive test, with the ram displacing at a constant 12mm/min until the sample is crushed as seen in Figure 7. Since this is a destructive test, it takes a larger load to fail the sample. Unfortunately, the required MTS load frame was out of service in the University of Arkansas testing lab, so the samples were shipped to the MeadWestvaco performance lab in Charleston, SC.



Figure 7 – IDT tested sample. (From <http://ntl.bts.gov>)

RESULTS AND DISCUSSION.

IDT Creep Data

The creep compliance curves for all the samples were combined and plotted at each of the three testing temperatures to get a better idea of the spread in results. Figures 6a, 6b and 6c depict these results.

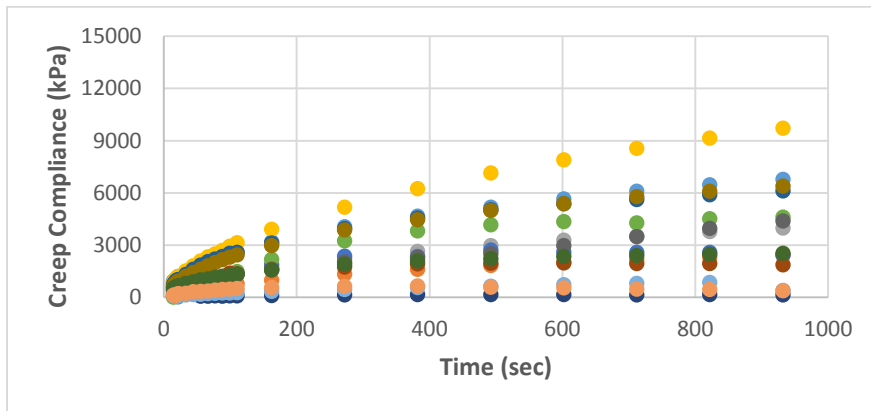


Figure 6a – Creep distribution at 0°C

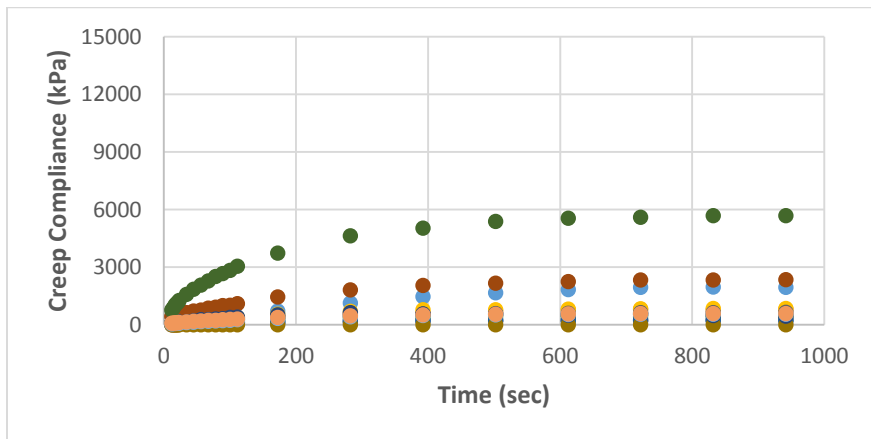


Figure 6b – Creep distribution at -10°C

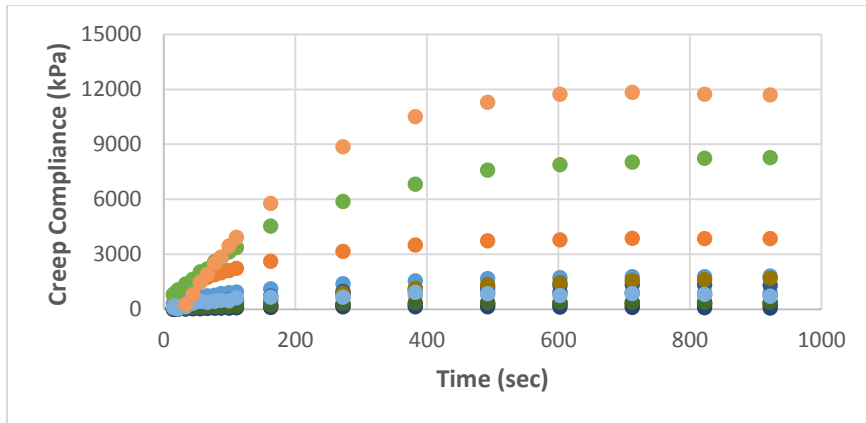


Figure 6c – Creep distribution at -20°C

At each temperature, the top and bottom curve were disregarded as outliers and trimmed out. Nevertheless, a wide range of curves is still notable among test results regardless of the testing temperature. All samples behaved as expected i.e. their creep compliance increased over time before leveling off. If the top set of data is disregarded at -10°C, and the top three sets of data are disregarded, the general trend of data indicates a decrease of creep, which is expected as the material behaves more elastically. In addition, the data “tightens” and the spread is decreased. It is common to only test three replicates, so it is rare to test such a large amount of similar samples in common practice and such a wide spread may not be as notable with a handful of specimens especially when outliers are trimmed out. Furthermore, the results obtained from these tests are quite atypical. In fact, the obtained results are orders of magnitude higher than expected. This anomaly could potentially be the subject of another experiment.

While comparing results from relatively similar specimens at the same temperature gives an insight into the variability in test results from the IDT creep test, contrasting them among test temperatures would unveil the effect, if any, of the test temperature on the test.

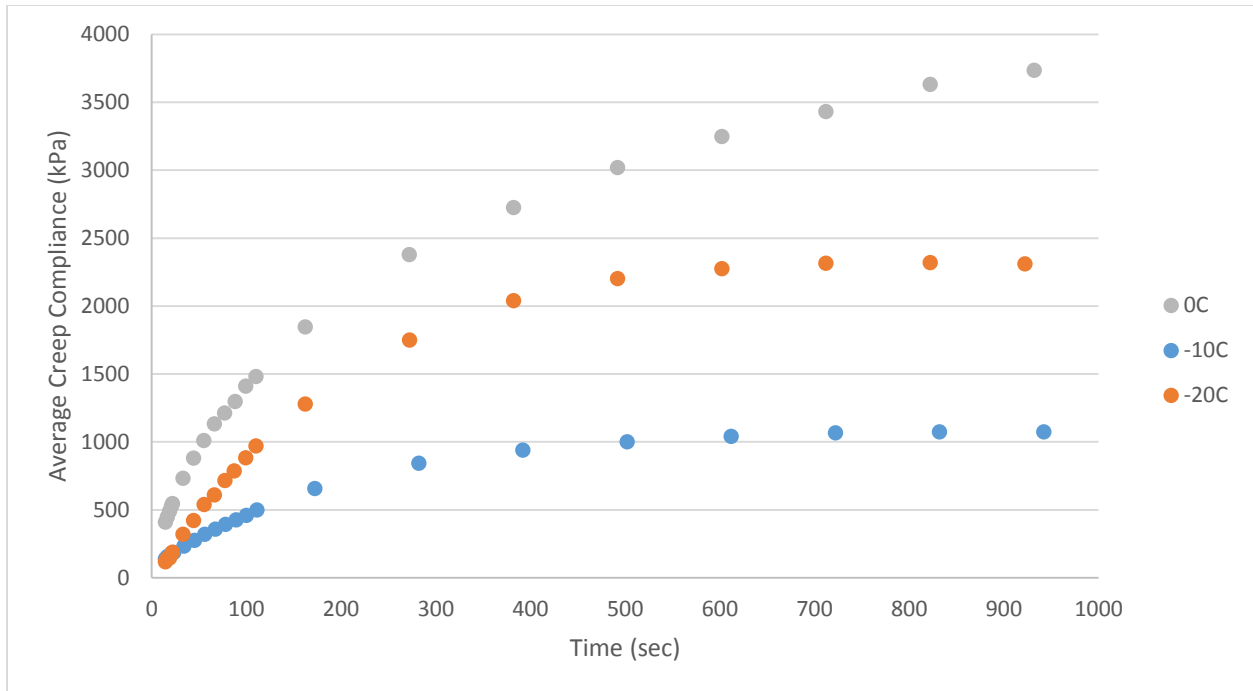


Figure 7 – Average creep compliance curves at all three temperatures.

As depicted in Figure 7, there is no apparent trend or relationship between the testing temperature and the average creep compliance. However, the highest creep compliance was expectedly reached at the warmest temperature of 0°C. At higher temperatures, the samples are more ductile and therefore more subject to creep forces. However, the second highest average creep compliance was reached at -20°C. This did not corroborate with the expected trend of a direct relationship between testing temperature and creep compliance. This might be indicative of some sort of deminishing return rule that effect they way temperature affects the samples being tested. The absence of obvious and notable relationship between temperature and creep compliance does not dismiss temperature as a factor in this experiment. A look at how it may affect other result properties such as the standard deviation and coefficient of variation would provide some insight into the matter.

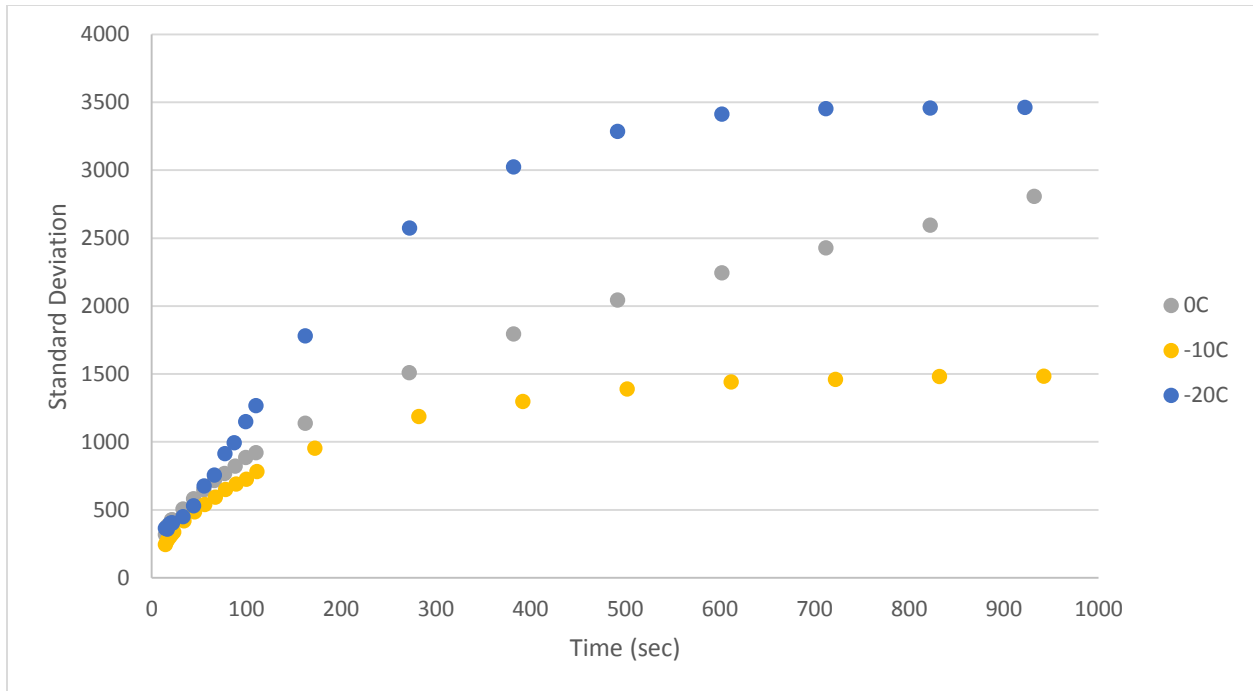


Figure 8 – Standard deviation of creep compliance.

Interestingly enough, the standard deviation curve has a similar shape as the actual creep compliance curve, as seen in Figure 8. It seems like the standard deviation grows over time before leveling off. This means that the results spread out more and more over time. Once again, there doesn't seem to be any strong relationship between the testing temperature and the standard deviation. Tests carried out at -20°C seem to have the the highest level of variability followed by the ones at 0°C and in last place -10°C . The high variability at -20°C might be the reason why the expected trend in average creep compliance with regards to the testing temperature was not observed. Another measure of variation is the results' coefficients of variability which are plotted in Figure 9.

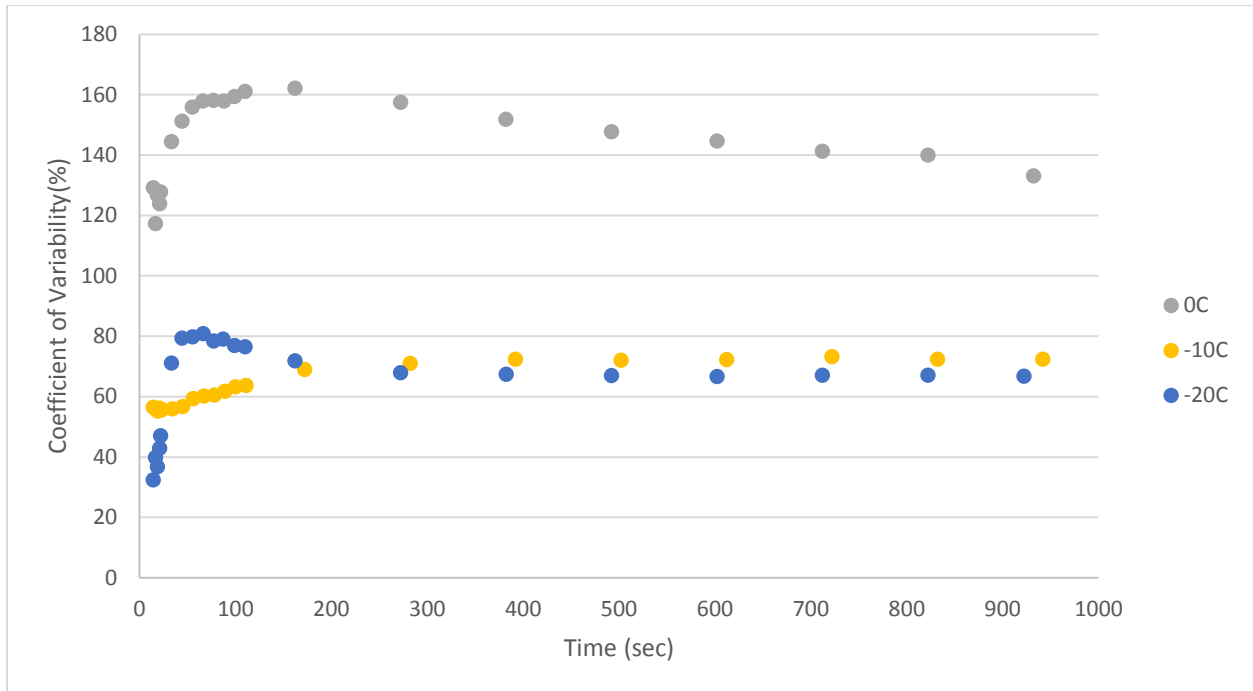


Figure 9 – Coefficient of variability at all three temperatures.

The upside of using this method to gauge the variability in results is the fact that it takes into account the magnitude of the data. As pointed out earlier, some specimens have higher average creep compliance values and comparing their coefficient of variability helps standardising the analysis. Other than a short spike at the beginning of the experiment, the coefficient of variability appears to remain relatively constant throughout the experiment. Furthermore, there is notable trend in these values among testing temperatures. It seems that lower temperatures tend to have lower values of coefficient of variability. It also seems that coefficients of variability get closer to each other as temperatures get lower. It is also worth pointing out that these values are much higher than anticipated and desired. Generally, COV values of 20% are ideal for this type of experiment. This reinforces the idea that these experiments produced highly variable results. A key question that should be asked is that assuming that this data is valid, perhaps there is more variability in asphalt concrete testing than previously thought. When only three samples are tested, it is easy to disregard one of the three sets of data if it appears to be an “outlier.” However, there is a chance that the highly heterogeneous nature of asphalt concrete may actually produce a significant range of data.

SCB Data

The SCB curves for all the samples were combined and plotted on the same graph to get a better idea of the spread in results, as seen in Figure 10. Similarly to the IDT creep test, the variability in the results was quite astonishing. Note that this data has not yet been shifted so the test “starts” at 0mm load cell stroke. The load cell stroke requires a seating load to be applied, so the initial load stroke is very rarely zero.

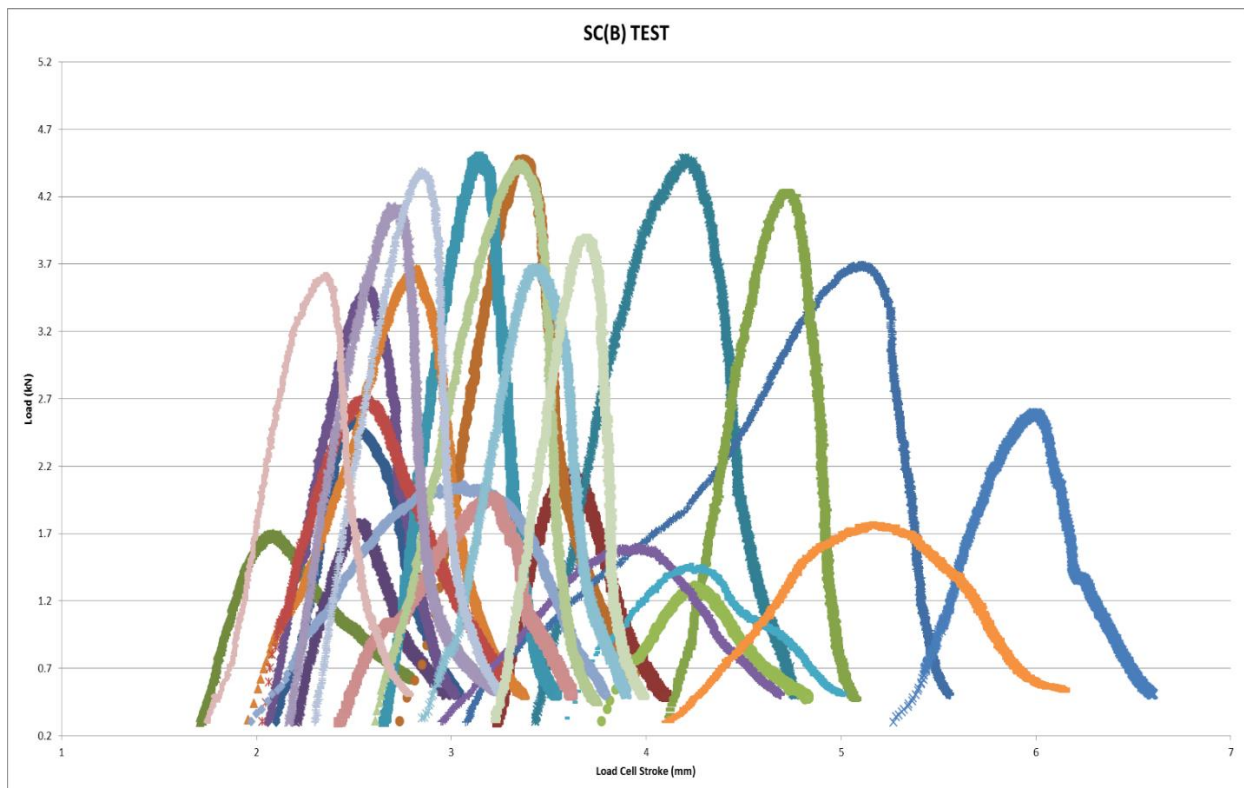


Figure 10 – SCB curves at -10°C

Similarly to the IDT creep test, this overall graph shows a very wide spread among specimens. Not only are the ranges of load cell stroke wide, but the peak loads also vary significantly. This is even more noticeable in this case since the spread occurs not only with the load values but also in the load cell stroke. Additionally, there doesn't seem to be a clear link between specimens achieving high creep compliance values and those with higher fracture energies. For example, at -10°C sample J27-01 had the second highest creep compliance curve whereas its SC(B) daughter specimens were ranked 16 and 18 in fracture energy. Vice versa, at -10°C sample J22-04 was ranked 12 (out of 14)

in the creep compliance curve, yet its daughter specimens were ranked first and second in fracture energy. Figure 11 combines and averages all these results.

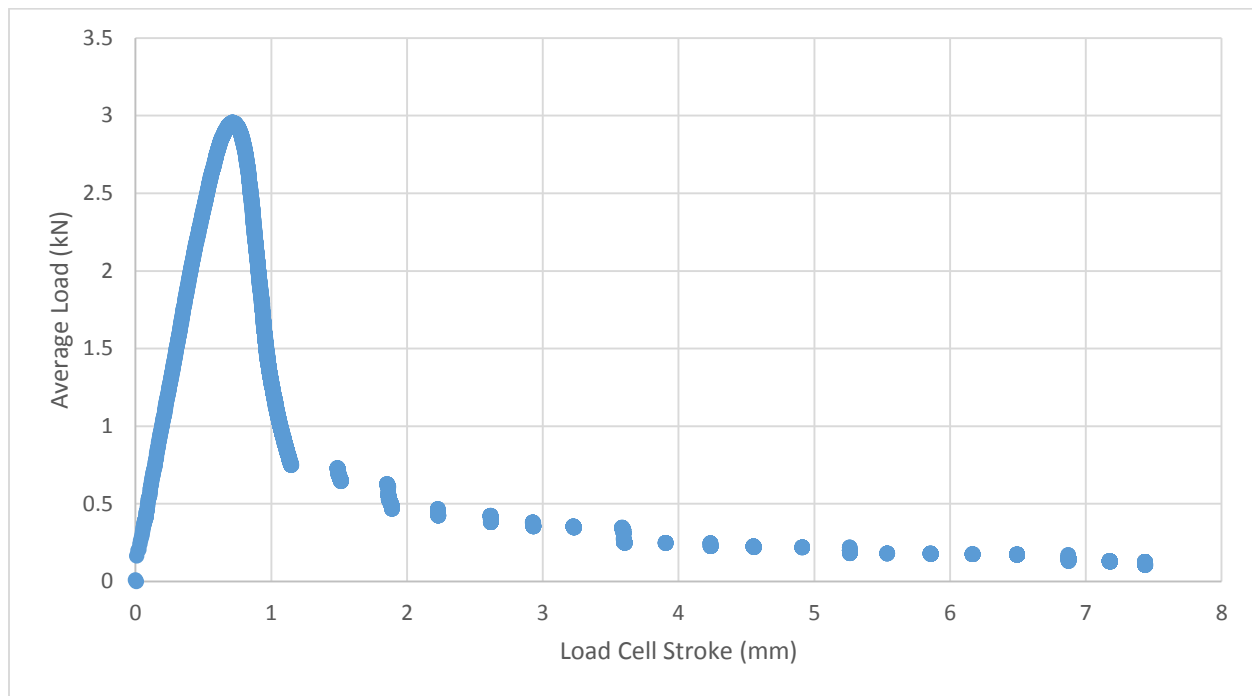


Figure 11 – Average SCB curve.

As depicted in the previous graph, the samples behaved typically under the SC(B) test. The specimens withstood the increasing pressure from the load cell until it culminated at approximately 3kN. At that point, the specimen failed and the load values dropped. The increase in pressure before the specimen fails and the drop after the specimen gives in are similar. The specimen does not crack faster. This behavior changes once the load cell stroke exceeds approximately 1mm. This is probably the point where the specimen has significant cracking.

Overall, however, the general shape of the fracture curve is representative of what other researchers have found. In order to gauge the variability in results from this test, the standard deviation and coefficient of variability were computed and plotted in Figures 12 and 13.

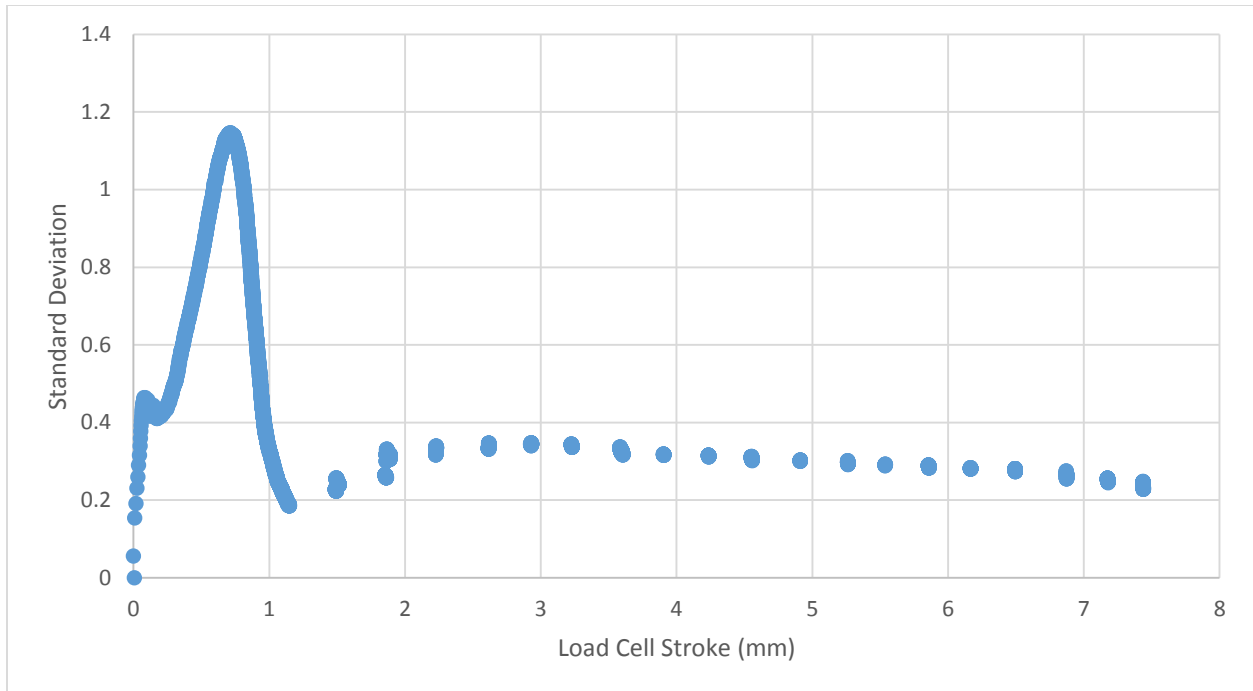


Figure 12 – Standard deviation of SC(B) curves

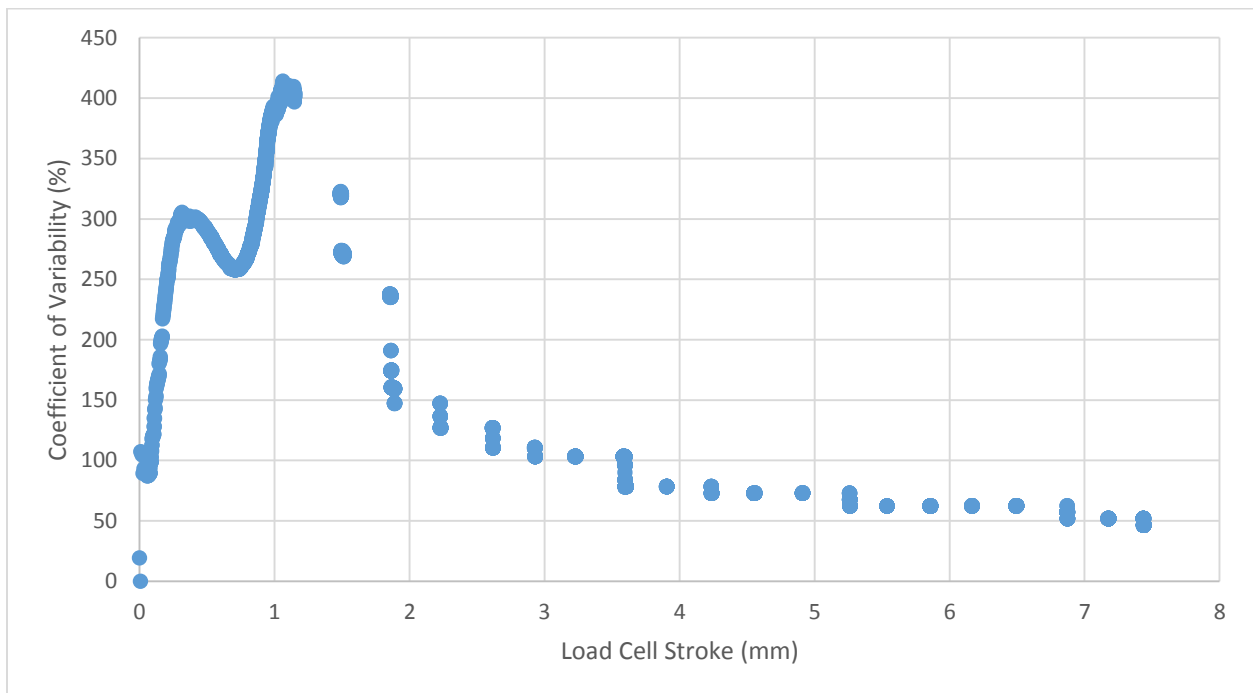


Figure 13 – Coefficient of Variability of SC(B) curves

Once again, the standard deviation and coefficient of variability plots are oddly similar to the actual test result curves. Furthermore, they both point to a great spread in results especially in the core portion of the test where most of the loading and

unloading occurs. Testing such a high number of samples has proven to result in a very wide range of results. In this particular case, COV values of 400% were attained. This variation also drops and levels out as the tests approach completion. A summary of fracture energy, or the area of the fracture curve divided by the crack ligament area, is shown in Table 2.

Table 2 – SC(B) Data Summary

Specimen	Fracture Energy (J/m ²)	Specimen	Fracture Energy (J/m ²)	Specimen	Fracture Energy (J/m ²)	Specimen	Fracture Energy (J/m ²)
J17-02A(1)	575.5	J22-04B(2)	2799.5	J27-01B(1)	444.2	J31-01A(2)	1024.4
J17-02A(2)	508.2	J22-05A(1)	1035.2	J27-01B(2)	857.1	J31-01B(1)	1045.7
J17-02B(1)	564.6	J22-05A(2)	863.3	J27-03A(1)	791.4	J31-01B(2)	1339.9
J17-02B(2)	404.4	J22-05B(1)	1033.1	J27-03A(2)	1267.0	J31-04A(1)	1082.2
J22-04A(1)	1515.6	J22-05B(2)	1395.7	J27-03B(1)	1208.9	J31-04A(2)	1002.1
J22-04A(2)	1175.4	J27-01A(1)	880.1	J27-03B(2)	701.7	J31-04B(1)	799.4
J22-04B(1)	2272.4	J27-01A(2)	862.2	J31-01A(1)	1336.4	J31-04B(2)	180.8
Average (kPa)				1034.5			
Stdev				538.3			
COV (%)				192.2			

Similar to the data collected in earlier sections, the COV is again extremely high for asphalt concrete testing. Again, it is thought that perhaps variability in asphalt concrete testing is quite prevalent, but the total number of samples traditionally tested may not completely capture that variability. This extreme variability in sample behavior could begin explaining why isolated sections of roadways prematurely deteriorate due to unknown causes. It could, in fact, be a function of the materials inherent significant variability. However, this is just one set of data from one set of samples, and this theory should be examined further.

IDT Strength

As mentioned earlier, the IDT strength test demands a much more powerful loading frame than the one used for the two previous tests. Unfortunately, the testing laboratory assisting with this last test was unable to get the testing done on time for the data to be processed and incorporated in this analyses. In future experiments, these results can be included for a more thorough and complete set of results.

CONCLUSION

Testing such a large amount of duplicates has proven to be eye opening. In common practice, performance tests are ran on few duplicates and outliers are usually disregarded as results of expectable experimental errors. To see this wide spread of results from an experiment conducted in a controlled environment indicates a possible lack of reliability in the current testing methods and numerical simulations based on or complementing these methods. After all, the samples were prepared using the same mix design. They were compacted using the same gyratory compactor, and were stored in the same environment. Further experimentation could unveil probable error sources or corroborate these results. In fact, data from the IDT strength test which, at the time this report was drafted, is being conducted by a third party, might be the first step in gaining this new perspective.

REFERENCES

American Association of State Highway and Transportation Official (2007). "Standard Method of Test for Determining the Creep Compliance and Strength of Hot Mix Asphalt (HMA) Using the Indirect Tensile Test Device" T 322-07, Washington, D.C.

American Association of State Highway and Transportation Official (2013). "Standard Method of Test for Determining the Fracture Energy of Asphalt Mixtures Using the Semicircular Bend Geometry (SCB)" TP 105-13, Washington, D.C.